Effect of Water Addition on Mitigation of Severe Accident Consequences in Nuclear Reactors

Abdelfatah Abdelmaksoud, M. M. Zaky

Reactors Department, Nuclear Research Center, Egyptian Atomic Energy Authority

Abstract

The injection of water to cool the degrading core is one of the main measures that is used to control the severe accidents in light water reactors. The interaction of water with the cladding material has a great impact on the accident progression. In the present work, an input deck is developed for RELAP-SCDAPSIM to study the loss of coolant scenarios in a nuclear fuel bundle at different operating pressures that include all pressure ranges for boiling water reactor (BWR), pressurized water reactor (PWR), and supercritical water reactor (SCWR). Effect of water addition on mitigating loss of bundle cooling is studied at different operating pressure and different simulation times. The bundle quenching with water shows that the quenching is associated with zirconium oxidation and generation of hydrogen. The mass of Hydrogen generation is reported for all the operating pressures and at different times of water addition. In this study both RELAP5 and SCDAP parts of the code are used in simulating the bundle transient scenarios. Both RELAP and SCDAP portion of the code calculates the behavior of the fuel bundle under normal and accident conditions. The SCDAP also includes models to treat the later stages of a severe accident including debris and molten fuel formation, debris/vessel interactions which is not available in RELAP5. The results of this study show that the time at which the bundle is quenched with water is of great importance. Quenching the bundle with water at the wrong time and/or values of water flow rate could result in an increase in bundle maximum temperature because of the associated exothermic energy as a result of the chemical interaction between water and cladding. The amount of released energy associated with the Hydrogen generation is reported for all the operating pressures and at different times of water addition.

Introduction

No industry is immune from accidents, but all industries learn from them. In civil aviation, there are accidents every year and each is meticulously analysed. The lessons from nearly one hundred

years' experience mean that reputable airlines are extremely safe. In the chemical industry and oil-gas industry, major accidents also lead to improved safety. There is wide public acceptance that the risks associated with these industries are an acceptable trade-off for our dependence on their products and services. With nuclear power, the high energy density makes the potential hazard obvious, and this has always been factored into the design of nuclear power plants. The few accidents have been spectacular and newsworthy, but of little consequence in terms of human fatalities. The novelty value and hence newsworthiness of nuclear power accidents remains high in contrast with other industrial accidents, which receive comparatively little news coverage.

In avoiding such accidents the industry has been very successful. In the 60-year history of civil nuclear power generation, with over 18,500 cumulative reactor-years across 36 countries, there have been only three significant accidents at nuclear power plants: Three Mile Island (USA 1979) where the reactor was severely damaged but radiation was contained and there were no adverse health or environmental consequences. Chernobyl (Ukraine 1986) where the destruction of the reactor by steam explosion and fire killed two people initially plus a further 28 from radiation poisoning within three months, and had significant health and environmental consequences.

Fukushima Daiichi (Japan 2011) where three old reactors (together with a fourth) were written off after the effects of loss of cooling due to a huge tsunami were inadequately contained. There were no deaths or serious injuries due to radioactivity, though about 19,500 people were killed by the tsunami. Of all the accidents and incidents, only the Chernobyl and Fukushima accidents resulted in radiation doses to the public greater than those resulting from the exposure to natural sources. The Fukushima accident resulted in some radiation exposure of workers at the plant, but not such as to threaten their health, unlike Chernobyl. Other incidents (and one 'accident') have been completely confined to the plant. The generation of hydrogen and the risk of hydrogen combustion, as well as other phenomena leading to containment over pressurization in the case of severe accidents, represent complex safety issues related to accident management. This publication concentrates on practical aspects of hydrogen risk related computational analysis and implementation of the risk mitigation measures for various reactor designs, with reference to documents already in existence

In this work, an input deck is developed for RELAP-SCDAPSIM to study a nuclear fuel bundle at different operating pressures that include all pressure ranges for boiling water reactor (BWR), pressurized water reactor (PWR), and supercritical water reactor (SCWR). The operating pressure

is allowed to change in the range of 1.9, 3.9, 6.9, 10.9, 19.9 23, and 25 MPa. Effect of water addition on mitigating loss of bundle cooling is studied at different operating pressure and different simulation times. The injection of water to cool the degrading core is the main measure used to control the severe accidents in light water reactors.

RELAP5 Modeling

All the thermal hydraulic calculation is performed by RELAP5. RELAP5 is a non-homogenous, non-equilibrium code that solves six hydrodynamic partial differential equations (conservation of mass, energy and momentum for liquid and gaseous phase). The fluid and energy flow paths are approximated by the one-dimensional stream tube and one-dimensional conduction model. The code contains system component models peculiar to pressurised water reactors (PWRs). In particular, a point neutronic model, pumps, turbines, steam generators, valves, separators and reactor control systems can be simulated. Additionally, it solves the conservation of mass for non-condensable gases. Also the equation of state for each phase, interphase mass and energy transfer and friction are calculated. An extensive wall heat transfer correlation package is available. The heat conduction in RELAP5 is one-dimensional. RELAP5/MOD3.2 code is based on a non-homogeneous and non-equilibrium model for the two-phase system that is solved by a fast, partially implicit numerical scheme to permit economical calculation of system transients.

The objective of the RELAP5 development effort from the outset was to produce a code that included important first-order effects necessary for accurate prediction of system transients but that was sufficiently simple and cost effective so that parametric or sensitivity studies were possible. The development of the models and code versions that constitute RELAP5 has spanned approximately 17 years from the early stages of RELAP5 numerical scheme development to the present. RELAP5 represents the aggregate accumulation of experience in modelling reactor core behaviour during accidents, two-phase flow processes, and LWR systems. The code development has benefited from extensive application and comparison to the experimental data in LOFT, PBF, Semiscale, ACRR, NRU, and other experimental programs.

SCDAP

SCDAP is a package of new models developed to support the severe accident phenomena calculation, which is not available in RELAP5. These models include an improved cladding deformation model, an improved high temperature cladding oxidation model, an oxide shattering model to compute the possible zircaloy cracking during the reflood phase of a transient, a simulator model to describe electrically heated rods, a model to describe the material interactions at high temperatures (eutectics interactions) and a model to describe melt formation and relocation. An improved radiation heat transfer model, fuel rod elements and control rod are also available. SCDAP also models shroud behaviour. The heat conduction in SCDAP elements is two-dimensional.

Two-dimensional heat conduction governing equation

In the two-dimensional cylindrical coordinate system, the integral form of the heat conduction equation for an isotropic solid continuum is:

$$\int_V \rho c_p \frac{\partial T}{\partial t} dV = \int_V \frac{1}{r} \frac{\partial}{\partial r}\left(rk \frac{\partial T}{\partial r}\right) dV + \int_V \frac{\partial}{\partial z}\left(k \frac{\partial T}{\partial z}\right) dV + \int_V Q_V dV + \int_S Q_S dS , \qquad (1)$$

where,

Q_V – volumetric heat source (nuclear, oxidation, W/m^3),

Q_S – surface heat flux (convective, radiative, W/m^2),

T – temperature at location (r, z) at time t where r and z are the radial and axial coordinates respectively (K),

ρc_p – volumetric heat capacitance (J/m^3K),

k – thermal conductivity ($W/m \cdot K$).

By applying the divergence theorem to the right-hand side of the integral form of the heat conduction equation, the following heat conduction governing equation is obtained:

$$\int_V \rho c_p(T,r,z)\frac{\partial}{\partial t}T(r,z,t)dV = \int_S k(T,r,z)\nabla T(r,z,t)dS + \int_V Q_V(r,z,t)dV + \int_S Q_S(r,z,t)dS\,. \qquad (2)$$

The equation (2) is solved using numerical methods. The result is temperature response of the fuel rod, control rod and shroud components.

Radiation model

RELAP5/SCDAPSIM has the capability of modelling radiation heat transfer between the various components in the core, including the coolant. The model calculates the radiation heat flux absorbed by the coolant and the radiant heat exchange between the surfaces of any vessel component (fuel rod, control rod, or shroud). The radiant heat exchange is a thermal boundary condition used in severe accident analysis of fuel rods, control rods, and flow shrouds. A mechanistic radiative heat transfer formulation, which accounts for each surface, the vapour, and each droplet, is complex. To develop such a detailed model for RELAP5/SCDAPSIM would not be cost effective. Instead, simplified models are used without sacrificing the accuracy of the results.

The radiation model presented here can be found in [39]. The solution method used is the net radiation method for an enclosure. Each component (fuel rod, control rod, or shroud) surface forms one side of an enclosure with n sides, and the enclosure is filled with coolant as in Fig (3.6). The radiation heat transfer equation for each surface describes radiation exchange with all surfaces (including itself if it radiates to itself) and absorption and emittance by the enclosed coolant. The n equations are solved simultaneously by a matrix inversion method to obtain the radiosity (the sum of emitted and reflected radiation energy rates) of each surface. The difference between the radiosity and incident energy from the surroundings gives the net heat flux to or from a surface. The algebraic sum of net heat flux corresponding to each surface gives the total radiation heat absorbed by the coolant.

Zircaloy oxidation model

The oxidation of zircaloy cladding is an important subject because the thermal and mechanical properties of oxidized zircaloy are significantly different than the unoxidized

properties. Moreover, the oxidation is highly exothermic. It can proceed rapidly enough at high temperatures to cause the reaction heat to significantly influence temperatures.

There are two types of oxidation processes regarding the temperature level – low temperature oxidation (573 K to 673 K), and high temperature oxidation (1239 K to 2100 K). Investigators [42] generally agree that oxidation of zirconium alloys by water in the temperature range from 573 K to 673 K proceeds by the migration of oxygen vacancies from the oxide metal interface through the oxide layer to the oxide coolant surface (and the accompanying migration of oxygen in the opposite direction). The vacancies at the metal oxide surface are generated by the large chemical affinity of zirconium for oxygen. Although the rate of oxidation is controlled in part by vacancy migration, the process of oxygen transfer from coolant to metal is not complete until the vacancy is annihilated by an oxygen ion at the oxide coolant surface. It is thus reasonable to expect the complex array of both bulk oxide properties effects and surface (coolant chemistry) effects that are reported in the literature.

Well-characterized data for out-of-pile oxidation are available from numerous experiments. The principal features of these data are:

- There is a transition between initial oxidation kinetics and later oxidation kinetics. The transition is a function of temperature and oxide layer thickness.
- The pre-transition oxidation rate is time dependent and inversely proportional to the square of the oxide thickness.
- The post-transition oxidation rate of a macroscopic surface is constant.

In spite of several past studies which have concentrated on the effects of dissolved oxygen, fast neutron flux, fast neutron fluence and gamma irradiation an adequate data base for a careful prediction of low temperature oxidation enhancements in reactor environments is not available.

Many of the complications observed with the low temperature oxidation are absent at high temperatures. For the high temperature range (1239 K to 2100 K), neither the heat flux nor the coolant chemistry has an important influence on the extent of oxidation. At these temperatures the coolant has become steam and oxidation proceeds much more rapidly than at normal LWR operating temperatures. Zircaloy normally has a body-centred cubic structure in this temperature range, called the beta phase, but the presence of oxygen causes two other possibilities. For oxygen

weight fractions around 0.04, a hexagonal close-packed phase called oxygen stabilized alpha Zircaloy is formed. If the oxygen concentration is greater than about 0.25 weight fraction, one of several zirconium dioxide structures is formed. Thus, high temperature oxidation of zircaloy in steam produces three layers: the ductile inner beta layer with minimal dissolved oxygen, an intermediate oxygen-stabilized alpha zircaloy layer, and a zirconium-dioxide layer near the zircaloy steam interface.

Zircaloy at high temperatures reacts rapidly with steam in the oxidation process described in the reaction

$$Zr + 2H_2O \rightarrow ZrO_2 + 2H_2 + 6.45 \cdot 10^6 \text{ J/kg Zr}. \quad (3)$$

This reaction shows strong exothermal behaviour of oxidation and the release of hydrogen. The exothermal characteristic of the reaction is a source of heat in the overall balance of energy and leads to increase of temperature. Under special circumstances, which involve temperatures and heat-up rates, the consequence can be catastrophic due to a self-sustain capacity of the reaction.

Oxidation of materials that form a protective oxide layer is frequently found to conform to the assumption that the rate determining process is the diffusion of oxygen atoms across the oxide. In this case, the rate of oxygen diffusion across the oxide layer is given by Fick's law

$$J_X = -D\frac{\partial N}{\partial X}, \quad (4)$$

where,

J_X – flux of oxygen atoms (atoms/m^{2}s),

D – diffusion coefficient (m^2/s),

N – concentration of oxygen atoms (atoms/m^3),

X – direction perpendicular to the oxide surface (m).

Problem Description

The bundle consists of 32 identical fuel rods. The bundle is 0.9144 m in height. The fuel rods in the bundle have an outer diameter of 9.63 mm and a pitch of 12.80 mm. The fuel pellet radius is 4.135 mm, inner cladding radius of 4.215 mm, and Outer cladding radius of 4.815 mm. Except for height, the design of the fuel rods is typical of PWR fuel rods. The flow area of the bundle of fuel rods is equal to 3.685×10^{-3} m^2. The bundle of fuel rods is surrounded by an adiabatic boundary through which no flow of heat occurs. The SCDAP/RELAP5 code represented the fuel bundle as eight equally sized axial nodes and eight equally sized hydrodynamic control volumes. The model include:

- Two identical bundles
  - 32 rods in 6X6 array – 0.91 m height
  - High decay heat – 58.5 Kw (2.0 Kw/m per rod)
- One bundle modeled using RELAP5 heat structure – 1D heat conduction only
- One bundle modeled using SCDAP fuel rod component – 2D heat conduction, oxidation, ballooning and rupture, material liquefaction
- Steady state calculation at supercritical pressure
- Severe transient at different operating pressure
- Water quenching
- 9 axial volumes in pipe
  - Pipe component 100 – SCDAP
  - Pipe component 300 – RELAP5
- Bundles water filled (550K)
- Inlet BC – water at 1.9, 3.9, 6.9, 10.9, 19.9 23, and 25 MPa. The initial temperature are 550, 500 K
- Outlet BC – Water at 1.89, 3.89, 6.89, 10.89, 19.89 22.9, and 24.9 MPa. The 550, 500 K
- Zirconium cladding is used for operating pressure of 1.9, 3.9, 6.9, 10.9, and 19.9 MPa.
- The proposed cladding material for supercritical reactor, alloy MA956 which has excellent strength at high temperatures due to dispersion of yttrium oxide (Y2O3) is used as a cladding material at operating pressure of 23, and 25 MPa. Composition of MA956: 74.5 wt% Fe, 20 wt% Cr, 4.5 wt% Al, 0.5 wt% Y2O3.

The mass flow that cools the bundle change with time as shown in Table (3.5) and the axial power peaking factor is shown in Table (3.6)

Table 3.5 mass flow that cools the bundle change with time

Time, s	Water flow rate (Kg/s)
0	1
50	1
100	0
900	0

Table (3) Axial power factor for each of the eight axial node

Axial node	1	2	3	4	5	6	7	8
Power factor	0.60	0.95	1.20	1.34	1.34	1.20	0.92	0.53

Figure (3.8) shoes the fuel bundle geometry and RELAP-SCDAPSIM nodaliziation for the bundle described above

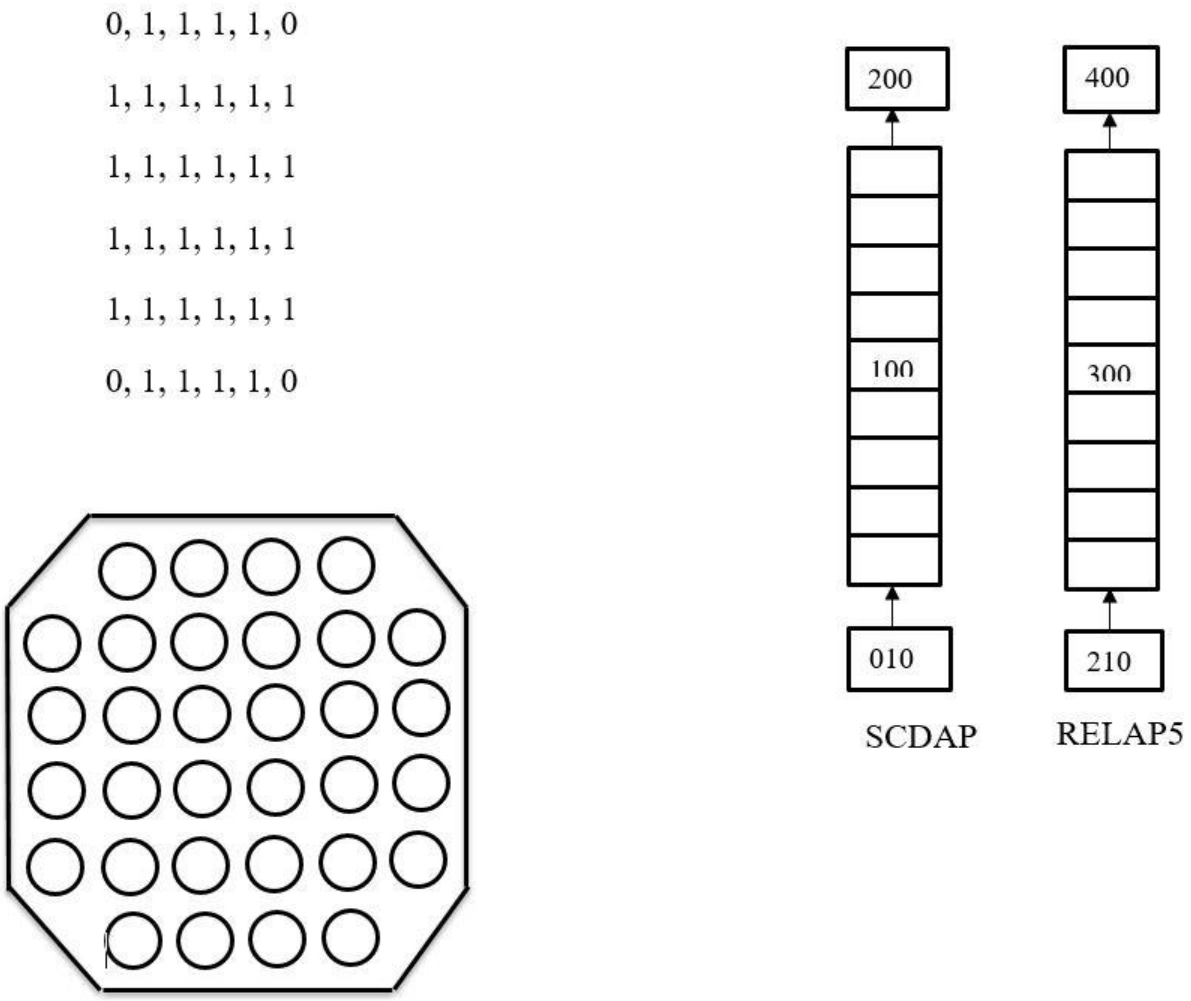

Fig. (8) Fuel bundle geometry and RELAP-SCDAPSIM nodaliziation

Effect of fuel bundle operating pressure

Before transient, it is assumed that the bundle under consideration has established steady-state conditions. Figures (4)- (5) shows the transient response of the clad and coolant temperature marching from the bundle initial conditions up to the steady state temperature profile for clad and coolant at different radial and axial nodes. The steady state solution for the clad temperature (httemp) and the coolant temperature (tempf) is shown in Table (1).

The transient scenarios start from the steady-state solution. The mass flow that cools the bundle change with time to test the bundle behavior under severe accident conditions. As the coolant flow rate decreases, transient heat up of the bundle in response to a reduced rate of coolant flow through the bundle start. Figure (6) shows the transient response of bundle clad temperature for bundle operating pressure of (1.9, 3.9, 6.9, 15.9, 19, 23, and 25 MPa). The operating pressure for the 32 fuel bundle under consideration is

Table 1 Steady state temperature for clad and coolant at different axial and radial node

Parameter	Temperature (^{0}C)
httemp -300100501	610.184
httemp -300100517	531.156
tempf -100010000	500.979
tempf -100020000	502.528
tempf -100030000	504.483
tempf -100040000	506.667
tempf -100050000	508.85
tempf -100060000	510.796

allowed to include all the pressure ranges for boiling water reactor (BWR), pressurized water reactor (PWR), and supercritical water reactor (SCWR). The bundle operating pressure has slightly small effect on fuel bundle maximum temperature for bundle pressure values lower than the critical pressure as shown in Fig. (6). The plateau in values of core maximum temperature (bgmct) at time greater than 200 is due to the melting that start to occur in zirconium cladding of the bundle. Although hydrogen production and its associated heat is generated after 200 s as shown in Fig. (7) and Fig. (8) respectively, the bgmct values doesn't increases sharply due to the latent heat associated with the melting of zirconium cladding inside the 32 fuel bundle. The small change in bundle maximum temperature (bgmct) with operating pressure change is not significant for operating pressures below the water critical pressure because of the same subcritical heat transfer correlation adopted in RELAP- SCDAPSIM at pressures less than the water critical pressure. The

bgmct values at operating pressure of 23 MPa and 25 MPa are lower than that at subcritical pressure at the end of the transient. The slight increase in bgmct

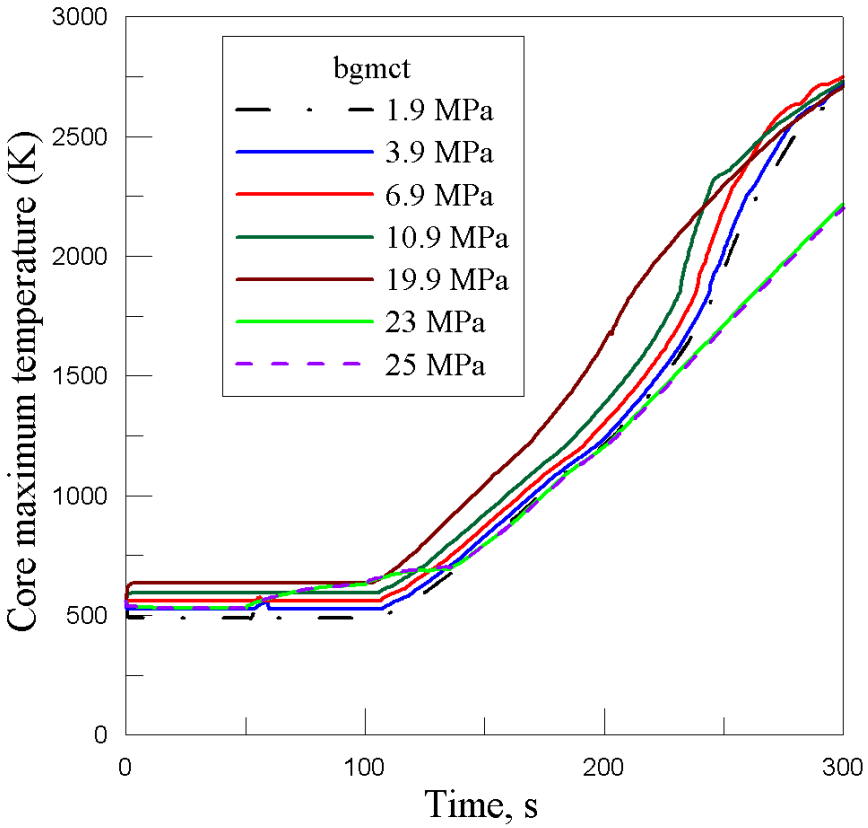

Fig.6 Transient response of bundle maximum temperature at different operating pressure

temperature at operating pressure of 23 MPa and 25 MPa in Fig. (4.26) between transient time of 60 s and 120 s is due to the variation in water properties massively around the critical point of water.

The identical supercritical bundle has no hydrogen generation as the zirconium cladding is replaced with alloy MA956 which is used for supercritical water cooled reactor cladding. SCDAP oxidation model predict almost no hydrogen generation with alloy MA956 as a cladding material as shown in Fig. (7). The supercritical bundle is more stable thermal-hydraulically than subcritical bundle with the same heat generation and geometry. There is no hydrogen production at operating pressures of 23 and 25 MPa and consequently its associated heat generation disappeared as depicted in Fig. (8). The hydrogen gas released due to oxidative reaction of zirconium with water, partly diffuses into the zirconium cladding alloy and forms zirconium hydrides. Figure (7)

shows the transient response of bundle hydrogen production at different operating pressure. For operating pressure values of 1.9, 3.9, 6.9, 15.9, 19, 23, and 25 MPa. The hydrogen production increases with increasing the operating pressure due to the augmentation that occur in the chemical reaction at high pressure and temperature. Further increasing the operating pressure to 19.9 MPa decreases the hydrogen production as depicted in Fig. (7). This is attributed to the limited diffusion of zirconium and water atoms at such a high pressure. One disadvantage of metallic zirconium is that in case of a loss-of-coolant transient as in the present study, zirconium cladding rapidly reacts with water steam at high temperature. Oxidation of zirconium by water is accompanied by release of hydrogen gas. This oxidation is accelerated at high temperatures. Metallic zirconium is then oxidized and hydrogen is produced. This exothermic reaction, although only occurring at high temperature. This reaction is

$$Zr + 2\ H2O \rightarrow ZrO2 + 2\ H2$$

responsible for a hydrogen explosion accident that can occur in case of huge amount of hydrogen generation. Hydrogen gas if vented into the reactor halls, the resulting explosive mixture of hydrogen with air oxygen will dentate. The resulting explosions will severely damage external buildings and at least the containment building of the reactor. That's why, It's recommended for zirconium cladding bundles to have catalyst-based recombination units installed to rapidly convert hydrogen and oxygen into water at room temperature before the explosive limit is reached. Figure (8) shows the transient response of bundle heat generation at different operating pressure. The trends of this figure follow the same trends in the previous one of hydrogen generation because this heat is generated from the exothermic reaction of hydrogen generation. There are two types of oxidation processes regarding the temperature level – low temperature oxidation (573 K to 673 K), and high temperature oxidation (1239 K to 2100 K). The oxidation of zirconium alloys by water in the temperature range from 573 K to 673 K proceeds by the migration of oxygen vacancies from the oxide metal interface through the oxide layer to the oxide coolant surface (and the accompanying migration of oxygen in the opposite direction). The vacancies at the metal oxide surface are generated by the large chemical affinity of zirconium for oxygen. Although the rate of oxidation is controlled in part by vacancy migration, the process of oxygen transfer from coolant to metal is not complete until the vacancy is annihilated by an oxygen ion at the oxide coolant surface. It is thus reasonable to expect the complex array of both bulk oxide properties effects and

surface (coolant chemistry) effects on the mass of hydrogen being generated during the accident progression.

For the high temperature range (1239 K to 2100 K), neither the heat flux nor the coolant chemistry has an important influence on the extent of oxidation. At these temperatures the oxidation proceeds much more rapidly than at normal LWR operating temperatures. Zircaloy normally has a body-centered cubic structure in this temperature range, called the beta phase, but the presence of oxygen causes two other possibilities. For oxygen weight fractions around 0.04, a hexagonal close-packed phase called oxygen stabilized alpha zircaloy is formed. If the oxygen concentration is greater than about 0.25 weight fraction, one of several zirconium dioxide structures is formed. Thus, high temperature oxidation of zircaloy in water produces three layers: the ductile inner beta layer with minimal dissolved oxygen, an intermediate oxygen-stabilized alpha zircaloy layer, and a zirconium-dioxide layer near the zircaloy steam interface.

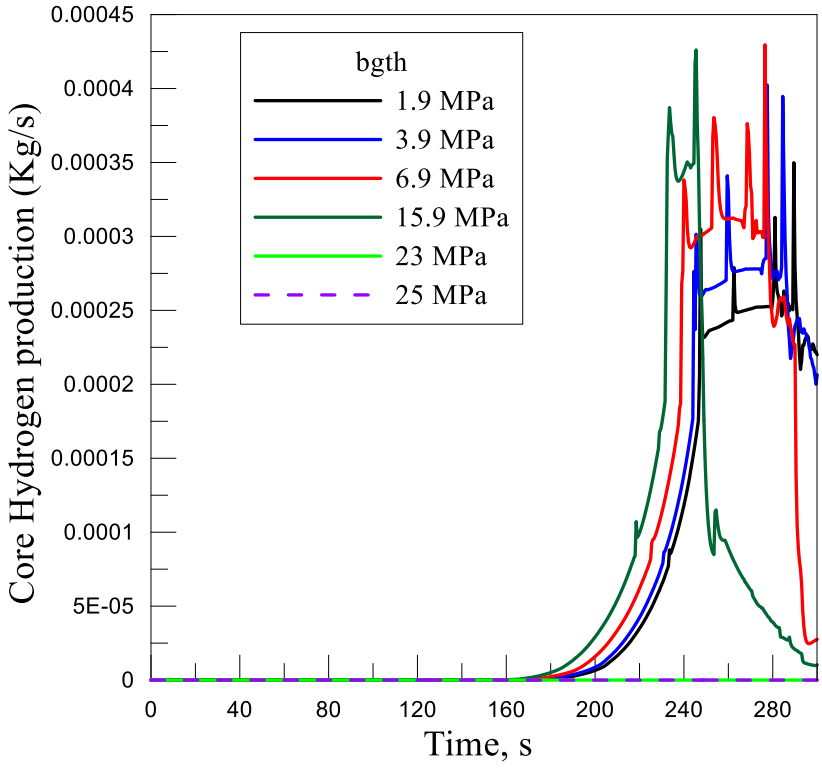

Fig.7 Transient response of bundle Hydrogen production at different operating pressure

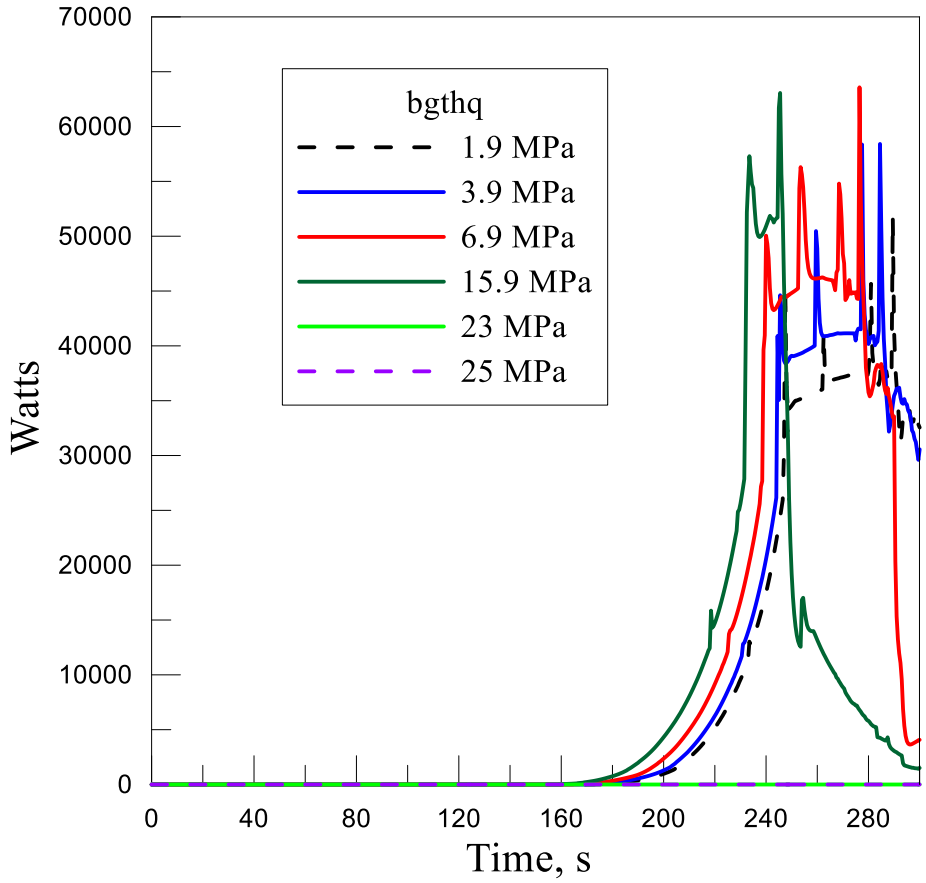

Fig.8 Transient response of bundle heat generation at different operating pressure

Figure (9) shows the transient response of bundle clad temperature at different operating pressure at mid-height of the bundle. The clad temperature at mid-height of the fuel bundle is maximum due to the cosine shape distribution of the nuclear heat generation of the fuel. The cosine shape profile of heat generation is described in chapter 3.

Figure (10) shows the transient response of bundle clad temperature predicted by RELAP and SCDAP at 6.9 MPa. A good a agreement between the temperature predicted by RELAP and SCDAP is achieved until the clad temperature reaches the zirconium melting point at 250 s. The deviation between the two results is due to the generated hydrogen and its accompanied heat production. RELAP5 doesn't contain models for hydrogen generation and material melting and solidification which exist only within SCDAP and then the deviation occur between RELAP and SCDAP when these models is invoked by the SCDAP portion of the code. That's why the two codes predict different temperatures after hydrogen production and bundle melting start in the bundle.

Effect of Water Addition on Mitigating Loss of Bundle Cooling

The injection of water to cool the degrading core is the main measure used to control the severe accidents in light water reactors. The bundle quenching with water shows that the quenching is associated with zirconium oxidation and huge amount of generation of hydrogen. Adding water to cool the bundle can result in bundle temperature to increase as will be shown in following results. Both RELAP and SCDAP portion of the code calculates the behavior of the fuel bundle under normal and accident conditions. The SCDAP also includes models to treat the later stages of a severe accident including debris and molten fuel formation, debris/vessel interactions which is not available in RELAP5. The latter SCDAP models are automatically invoked by the code as the damage in the bundle progresses. Figures (11- (12) shows the transient response of bundle clad temperature with water quenching at quenching time of (250, 260, and 270 sec) and pressure of (1.9, 3.9, 6.9 MPa, 15.9, 19, 23, and 25 MPa). The water addition transients is conducted at wide range of operating pressures. The operating pressure include all the pressure ranges for boiling water reactor (BWR), pressurized water reactor (PWR), and supercritical water reactor (SCWR). The time at which water quenching occur is of great importance. Water quenching should be used prior to the zirconium cladding reach its melting temperature. The addition of water for the purpose of mitigating accident and maintaining fuel bundle integrity at the wrong timing during the accident progression can lead to increasing the fuel temperature. This explain the reason of having maximum cladding temperature increases with increasing the quenching time more than 250 s which is the time at which zirconium start to catch its melting temperature as shown below. Addition of water after zirconium cladding melting increases the rate at which hydrogen production generate inside the bundle and consequently the associated the heat generation increases from the exothermic chemical reaction between water and zirconium.

Figs.(14), (15), (16), (17) and (18) shows the transient response of bundle hydrogen production with water quenching at 250, 260, 270 sec and pressure of (1.9, 3.9, 6.9, 15.9, and 19 MPa). The mass of hydrogen production increases with increasing the operating pressure because the kinetics of the chemical reaction between zirconium and water is being enhanced in such a high pressure and temperature environment. With increasing the temperature and pressure the diffusion of water and zirconium atoms and the probability of the chemical reaction increases. The bundle maximum temperature for quenching time of 250 s are 2151.35 C^o, 2235.81 C^o , 2459.46

C^o , 2521 .7 C^o, 2607.16 C^o , 1735.93 C^o , 1723.31 C^o for pressure of 1.9, 3.9, 6.9, 15.9, 19, 23, and 25 MPa respectively as shown in Table 4.2. The values of maximum bundle temperature decreases with increasing the operating pressure at which quenching water is accomplished. The same holds true for quenching times of 260 s and 270 s.

Table 2 Fuel bundle maximum temperature as function of quenching time, operating pressure and time of maximum temperature.

Quenching time (sec)	Pressure (MPa)	bgmct (^{0}C)	Time of max. temperature
250	1.9	2151.35	254
260	1.9	2507.49	265.5
270	1.9	2849.02	295
250	3.9	2235.81	255.5
260	3.9	2528	265.5
270	3.9	2762.06	278.5
250	6.9	2459.46	255.5
260	6.9	2625.95	265
270	6.9	3150.38	283
250	15.9	2521.7	252.5
260	15.9	2696.75	262.5
270	15.9	2848.65	273
250	19.9	2607.16	252
260	19.9	2765.65	262
270	19.9	3177.68	287.5
250	23	1735.93	252.5
260	23	1838.17	262
270	23	1937.48	272
250	25	1723.31	252.5
260	25	1824.81	262
270	25	1927.62	272.05

Figures (16)- (17) shows the effect of water quenching in mitigating the accident consequences for bundle operating pressure higher than the critical pressure. The amount of hydrogen production for supercritical bundle and the associated heat generation is almost zero because of replacing the zirconium cladding with the proposed cladding for supercritical reactor.

The supercritical bundle is more thermal hydraulic stable in mitigating the accident consequences due to the absence of any hydrogen generation for alloy MA956 as cladding. The highly corrosive environment of supercritical water will be the dominating challenge. The maximum bundle temperature for supercritical bundle is much lower than that at subcritical pressure. Supercritical bundle takes the advantage of massive change in water properties at supercritical pressure. Natural convection cooling is enhanced for the supercritical bundle, Both the effect of heat transfer enhancement due to supercritical pressure and natural convection combine together to make the supercritical reactor more stable thermal hydraulically at severe accident conditions. The ability of supercritical bundles at 23 and 25 MPa in mitigating accident consequences is much higher than the ones at pressure ranges at subcritical pressure range. The current water quenching scenarios to figure out the proper severe accident management strategy to identify the areas for the potential improvements including core cooling strategy, containment venting, hydrogen control, depressurization of primary system, and proper indication of event progression. Prevention of fuel bundle from reaching its melting temperature during severe accident mitigation is of great importance as the molten fuel debris relocated into the lower head filled with water could lead to a re-criticality if there is a source of neutrons.

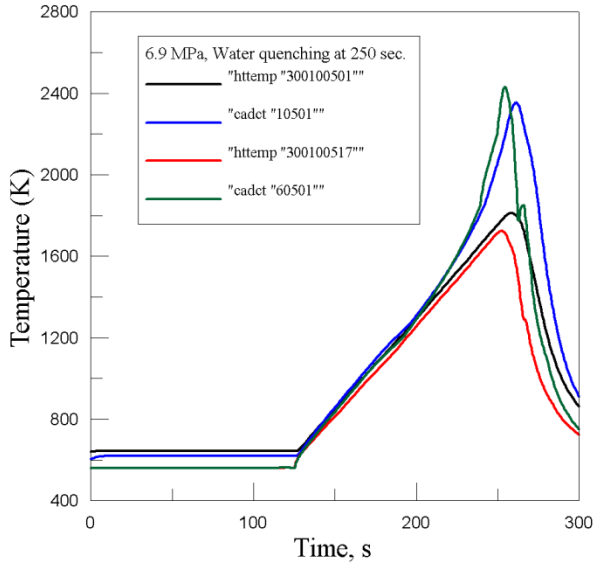

Fig.(16) Transient response of bundle clad temperature with water quenching at 250 sec and 6.9 MPa

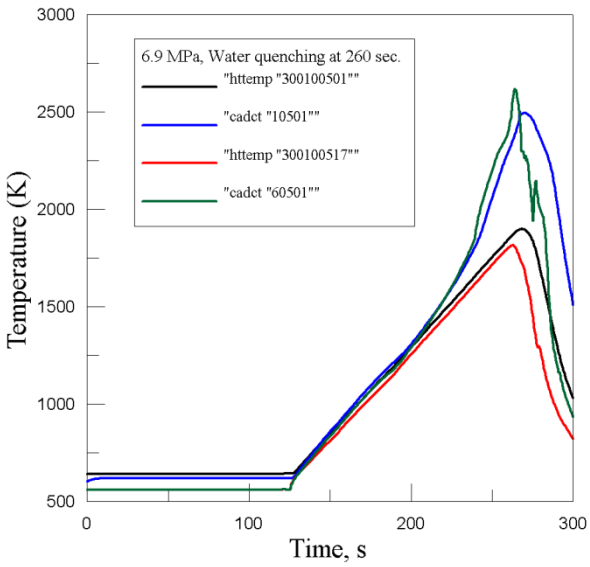

Fig.(17) Transient response of bundle clad temperature with water quenching at 260 sec and 6.9 MPa

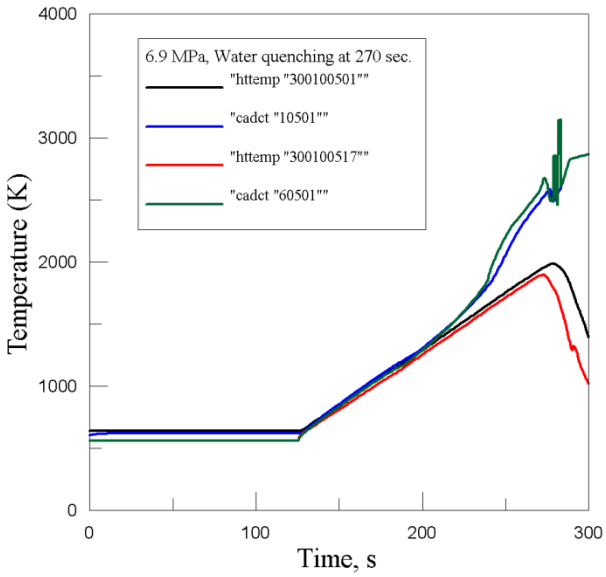

Fig.(18) Transient response of bundle clad temperature with water quenching at 270 sec and 6.9 MPa

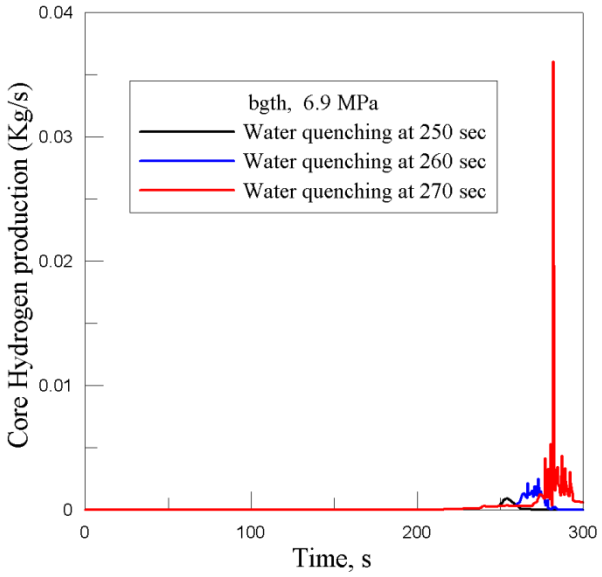

Fig.(19) Transient response of bundle Hydrogen production with water quenching at 250, 260, 270 sec and 6.9 MPa

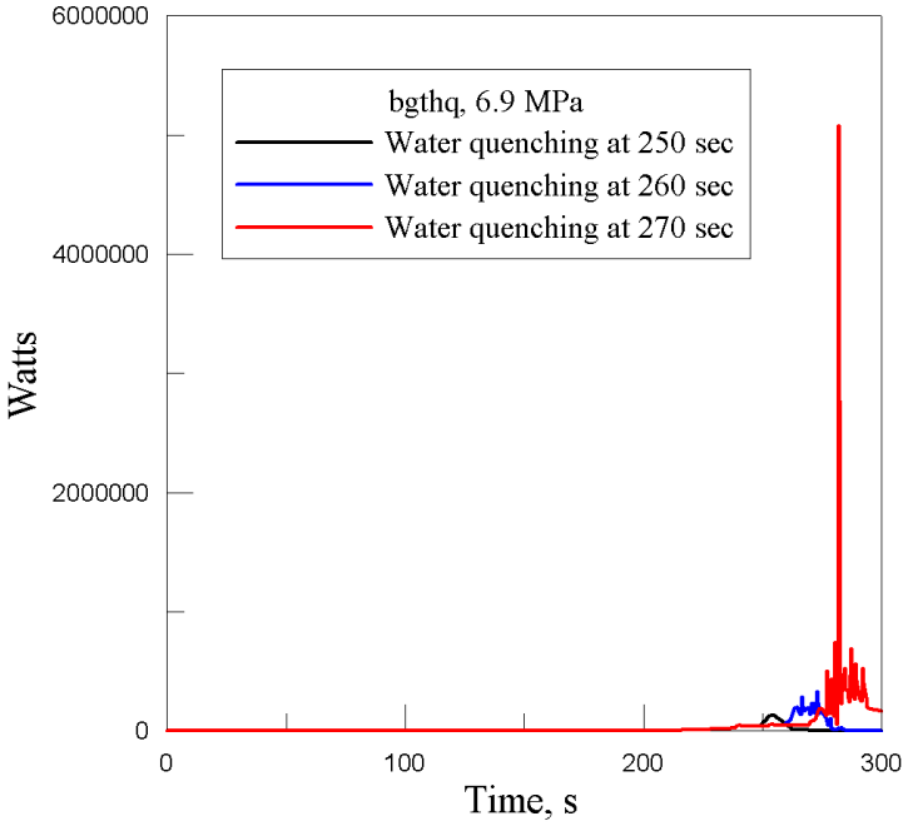

Fig.(20) Transient response of bundle Hydrogen production heat generation with water quenching at 250, 260, 270 sec and 6.9 MPa

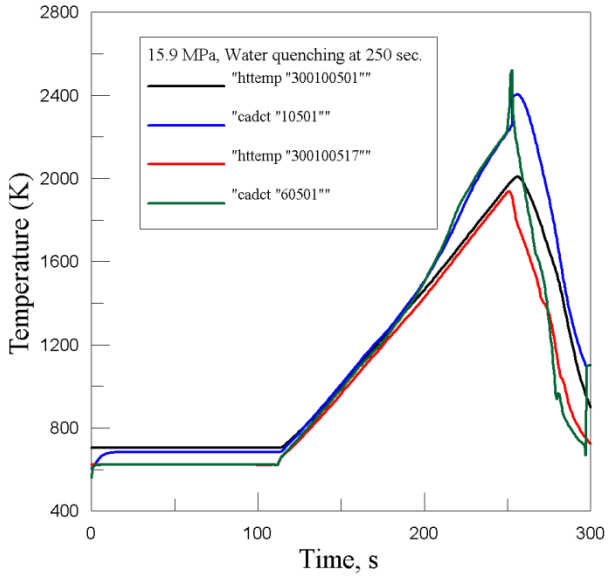

Fig.(21) Transient response of bundle clad temperature with water quenching at 250 sec and 15.9 MPa

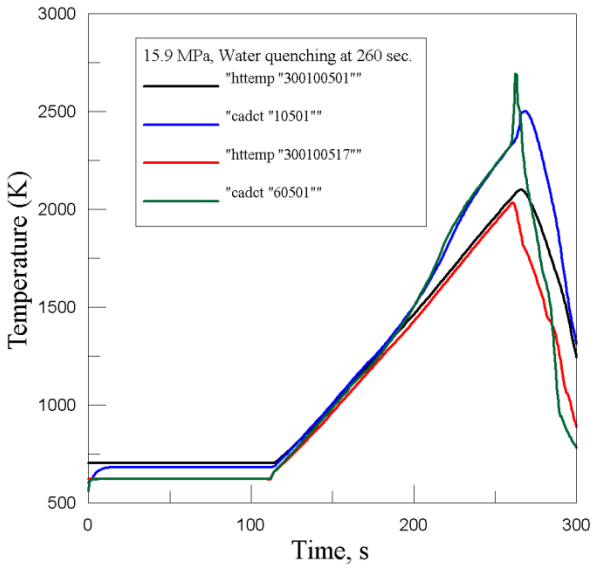

Fig.(22) Transient response of bundle clad temperature with water quenching at 260 sec and 15.9 MPa

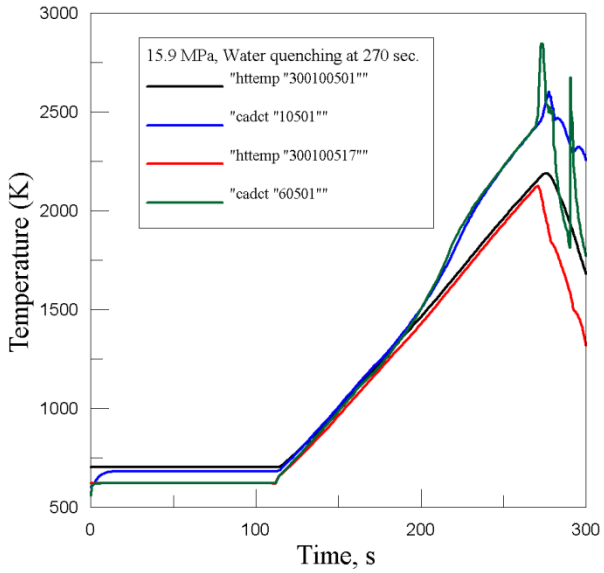

Fig.(23) Transient response of bundle clad temperature with water quenching at 270 sec and 15.9 MPa

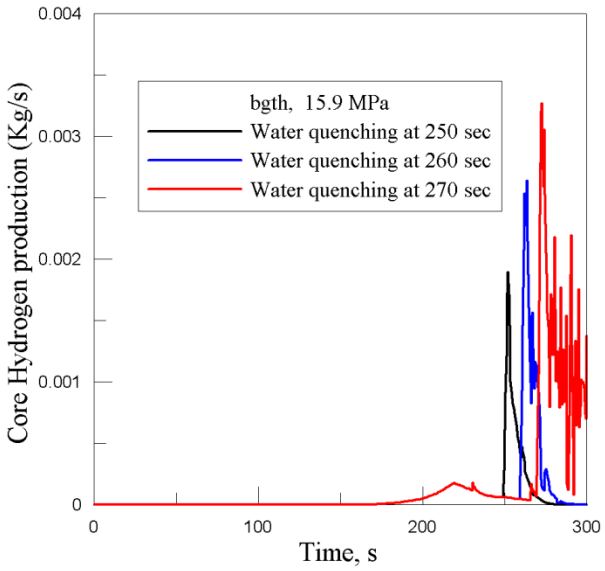

Fig.(24) Transient response of bundle Hydrogen production with water quenching at 250, 260, 270 sec and 15.9 MPa

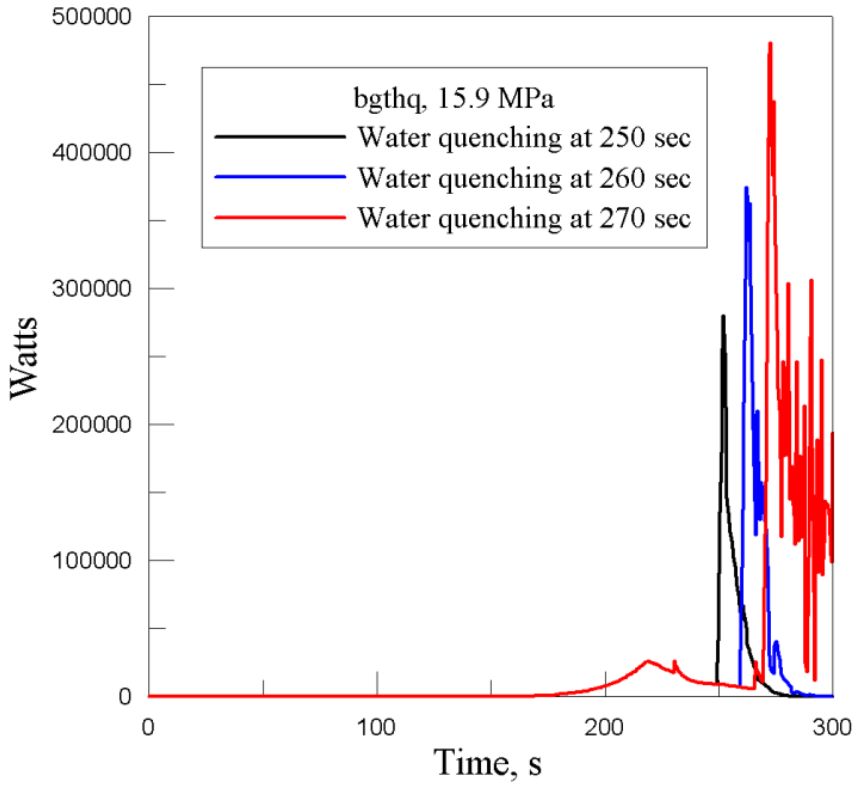

Fig.(25) Transient response of bundle Hydrogen production heat generation with water quenching at 250, 260, 270 sec and 6.9 MPa

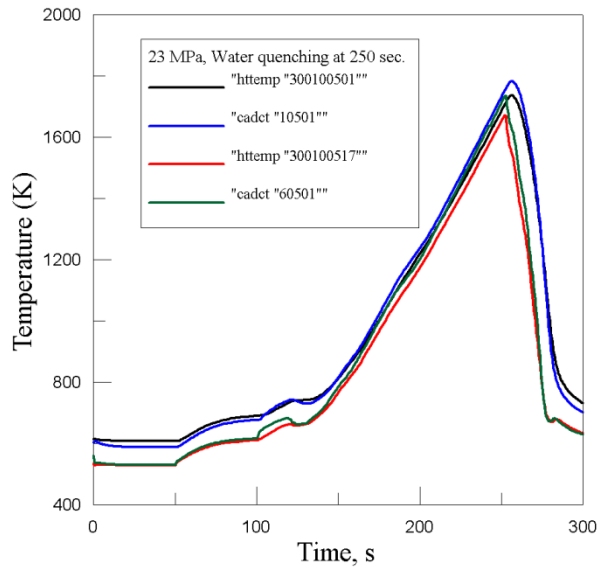

Fig.(26) Transient response of bundle clad temperature with water quenching at 250 sec and 23 MPa

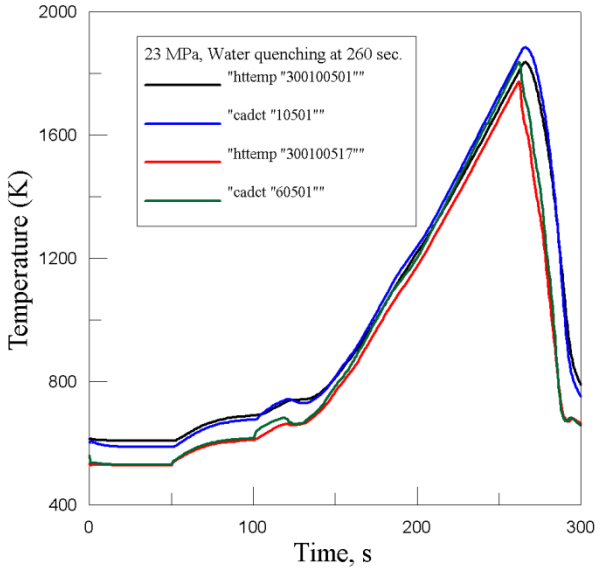

Fig.(27) Transient response of bundle clad temperature with water quenching at 260 sec and 23 MPa

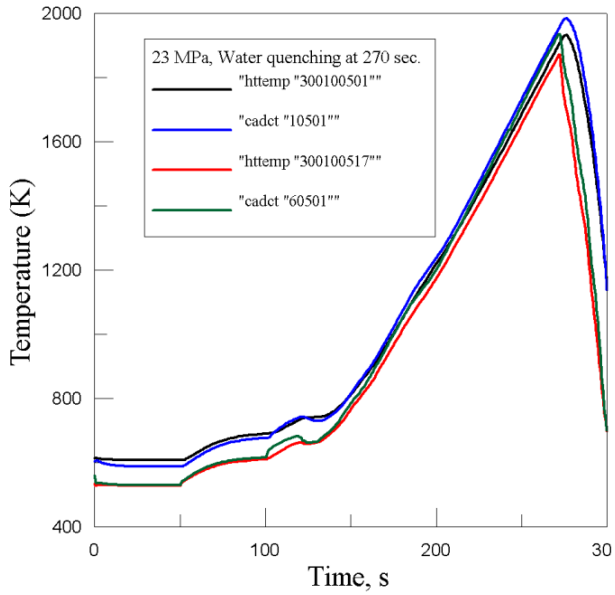

Fig.(28) Transient response of bundle clad temperature with water quenching at 270 sec and 23 MPa

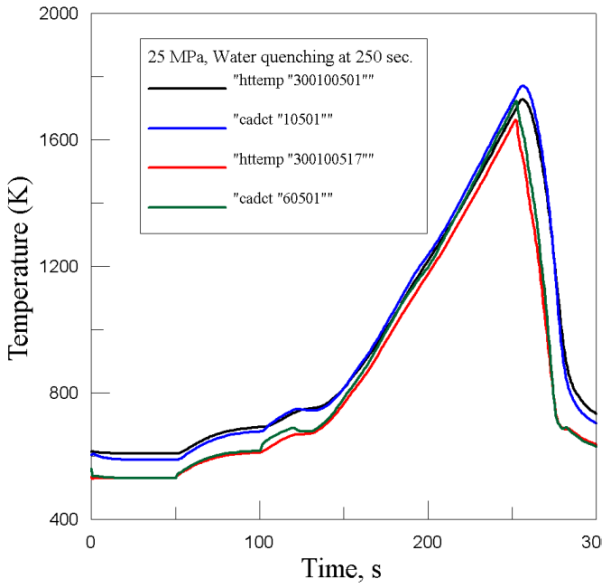

Fig.(29) Transient response of bundle clad temperature with water quenching at 250 sec and 25 MPa

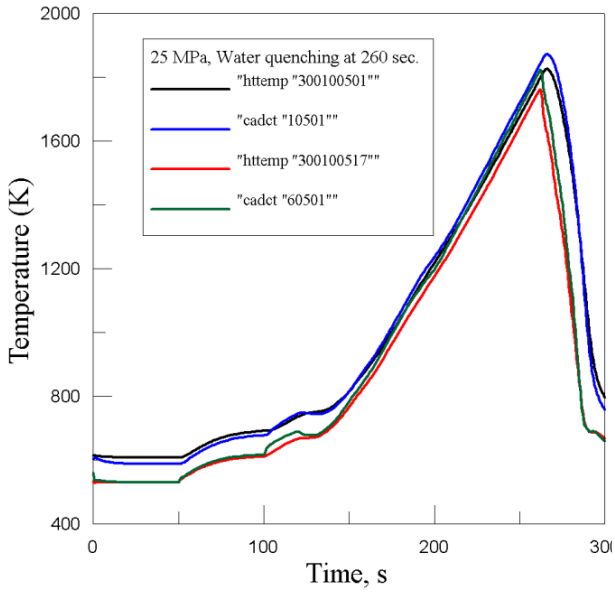

Fig.(30) Transient response of bundle clad temperature with water quenching at 260 sec and 25 MPa

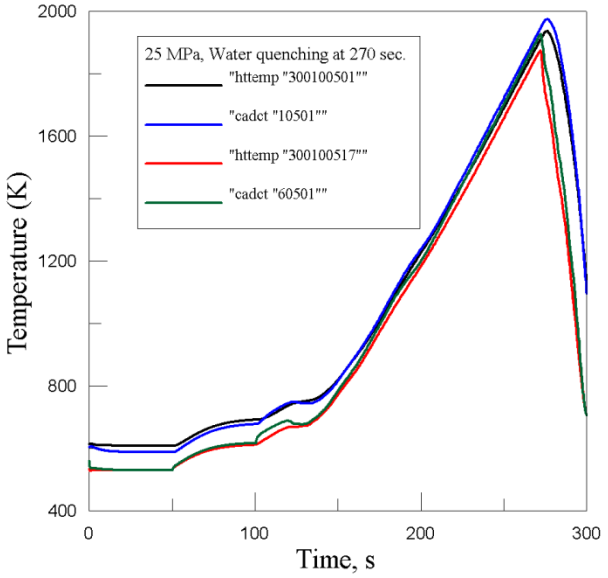

Fig.(31) Transient response of bundle clad temperature with water quenching at 270 sec and 25 MPa

4.6 Effect of decay power values

Decay heat is the heat released as a result of radioactive decay. This heat is produced as an effect of radiation on materials: the energy of the alpha, beta or gamma radiation is converted into

the thermal movement of atoms. Decay heat continues to be generated after the reactor has been shut down and nuclear chain reactions have been suspended. The decay heat play an important role in nuclear reactor accident scenarios. The bundle under consideration is studied for three different values of decay heat in order to show the effect of decay heat values in driving the accident and on the values of hydrogen production.

The fuel bundle under consideration is being analyzed for different values of heat generation. The low, reference, and high values of heat generation per bundle are 70 KW, 50 KW, and 30 KW per bundle respectively. Figures (4.72)- (4.74) shows the maximum bundle temperature for the three values of decay power. The bgmct values decreasing with decreasing the values of decay power. The bundle hydrogen production decreases with decreasing the decay power as shown in Figures. (4.75)- (4.77). The supercritical bundle can negotiate with high decay power more than that at lower or subcritical pressure as depicted from the bgmct values corresponding to supercritical pressures in the following figures.

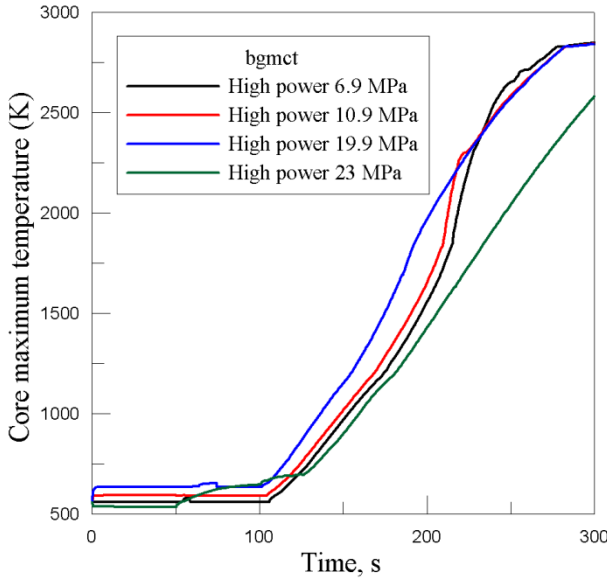

Fig.(32) Transient response of bundle maximum temperature at different operating pressure, 70 KW/ bundle

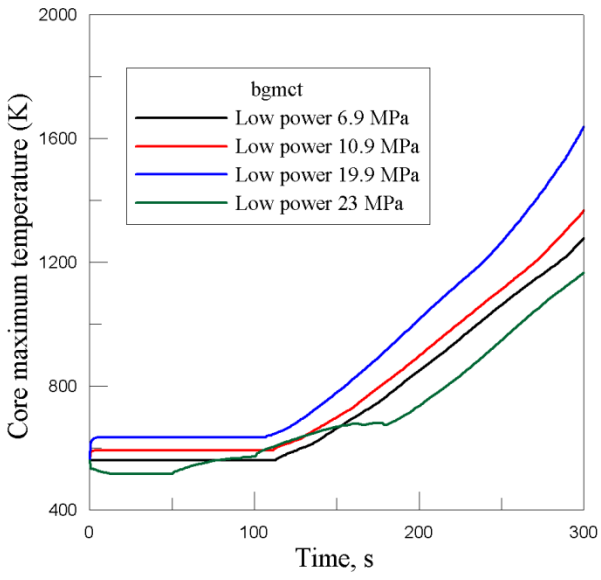

Fig.(33) Transient response of bundle maximum temperature at different operating pressure, 30 KW/ bundle

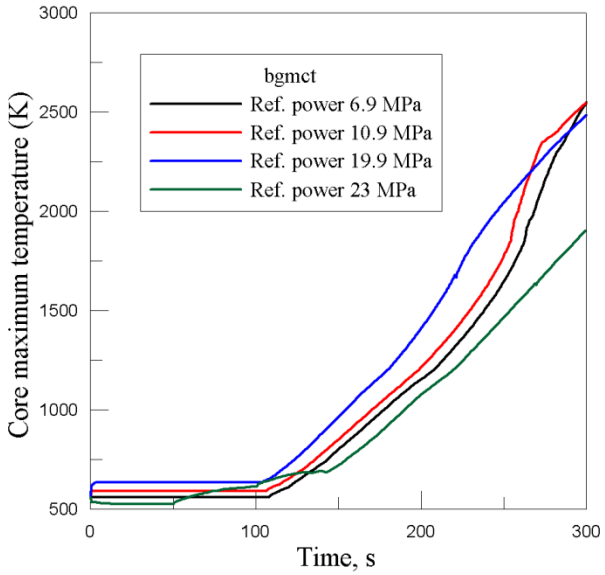

Fig.(34) Transient response of bundle maximum temperature at different operating pressure, 50 KW/ bundle

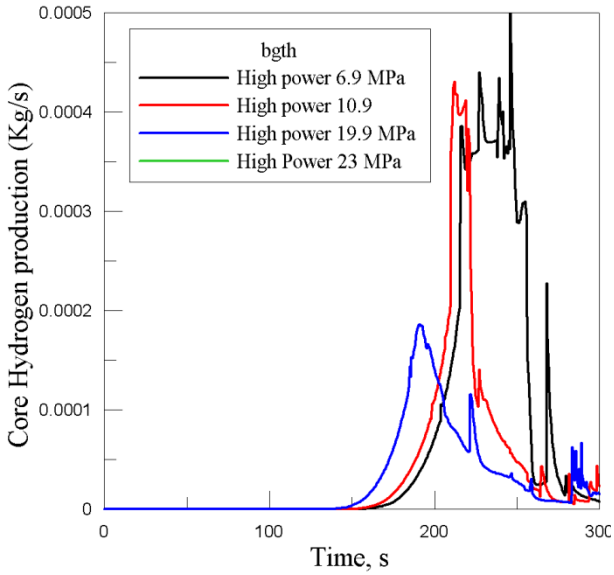

Fig.(35) Transient response of Hydrogen generation at different operating pressure, 70 KW/ bundle

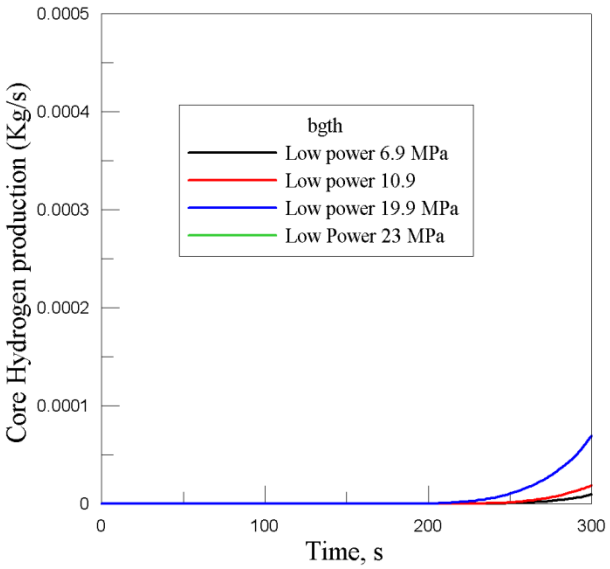

Fig.(36) Transient response of Hydrogen generation at different operating pressure, 30 KW/ bundle

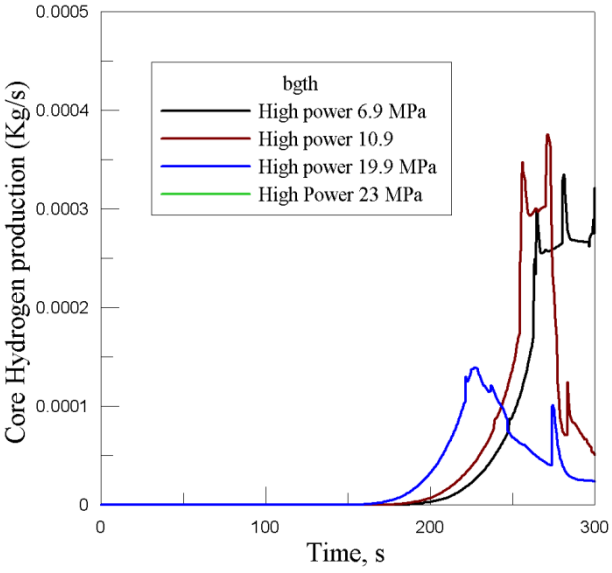

Fig.(37) Transient response of Hydrogen generation at different operating pressure, 50 KW/ bundle

Conclusion

In this work, an input deck is developed for RELAP-SCDAPSIM to study a nuclear fuel bundle at different operating pressures that include all pressure ranges for boiling water reactor (BWR),

pressurized water reactor (PWR), and supercritical water reactor (SCWR). The operating pressure is allowed to change in the range of 1.9, 3.9, 6.9, 10.9, 19.9 23, and 25 MPa. Effect of water addition on mitigating loss of bundle cooling is studied at different operating pressure and different simulation times. The injection of water to cool the degrading core is the main measure used to control the severe accidents in light water reactors. The bundle quenching with water shows that the quenching is associated with zirconium oxidation and generation of hydrogen. Hydrogen generation is reported for all the operating pressures and at different times of water addition.

The following are the main findings of this thesis work.

1. A RELAP5 input model is developed to simulate a typical fuel bundle under wide range of operating pressure ranging from 2 MPa up to 35 MPa.
2. Effect of water addition on mitigating loss of bundle cooling is studied at different operating pressure and different simulation times.
3. The bundle under consideration is studied for three different values of decay heat in order to show the effect of decay heat values in driving the accident and on the values of hydrogen production.
4. Hydrogen generation is studied at all pressure ranges. Almost no hydrogen production is associated with supercritical bundle proposed cladding.
5. Bundles at supercritical pressure shows superior thermal hydraulic performance in mitigating accident consequences compared to that at subcritical pressure.

References

1. Alekseev, G.V., Silin, V.A., Smirnov, A.M., Subbotin, V.I., 1976. Study of the thermal conditions on the wall of a pipe during the removal of heat by water at a supercritical pressure. High Temp. 14, 683–687.

2. Griem, H., 1996. A new procedure for the prediction of forced convection heat transfer at near-and supercritical pressure. Heat Mass Transf. 31, 301–305.

3. Mokry, S., Pioro, I., Kirillov, P., Gospodinov, Y., 2010. Supercritical-water heat transfer in a vertical bare tube. Nucl. Eng. Des. 240, 568–576.

4. Pan, J., Yang, D., Dong, Z.C., Zhu, T., Bi, Q.C., 2011. Experimental investigation on heat transfer characteristics of water in vertical upward tube under supercritical pressure. Nucl. Power Eng. 32, 75–79 (in Chinese).

5. Shitsman, M.E., 1968. Temperature conditions in tubes at supercritical pressures. Therm. Eng. 15 (5), 72–77.

6. Swenson, H.S., Carver, J.R., Kakarala, C.R., 1965. Heat transfer to supercritical water in smooth-bore tubes. J. Heat Transfer, Trans. ASME, Ser. C 87, 477–484.

7. Vikhrev, Yu.V., Barulin, Yu.D., Kon'kov, A.S., 1967. A study of heat transfer in vertical tubes at supercritical pressures. Therm. Eng. 14, 116–119.

8. Yamagata, K., Nishikawa, K., Hasegawa, S., et al., 1972. Forced convective heat transfer to supercritical water flowing in tubes. Int. J. Heat Mass Transf. 15, 2575–2593

9. Zhu, X., Bi, Q., Yang, D., Chen, T., 2009. An investigation on heat transfer characteristics of different pressure steam-water in vertical upward tube. Nucl. Eng. Des. 239, 381–388.

10. IAEA. Safety glossary. Terminology used in nuclear safety and radiation protection. 2007.

11. Zhang YP, Niu SP, Zhang LT, Qiu SZ, Su GH, Tian WX. A review on analysis of LWR severe accident. J Nucl Eng Radiat Sci 2015;1, 041018.

12. Bromet EJ, Parkinson DK, Dunn LO. Long-term mental health consequences of the accident at Three Mile Island. Int J Ment Health 1990;19(2):48e60.

13. Ministry of Chernobyl (MinChernobyl). Ten years after the accident at the Chernobyl NPP. National Report of the Ukraine. Kiev. 1996.

14. Povinec PP, Hirose K, Aoyama M. Fukushima accident: radioactivity impact on the environment. Newnes; 2013.